

A Theoretical Analysis of the Free-Energy Profile of the Different Pathways in the Alkaline Hydrolysis of Methyl Formate In Aqueous Solution

Josefredo R. Pliego, Jr. and José M. Riveros*^[a]

Abstract: The free-energy profile for the different reaction pathways available to the hydroxide ion and methyl formate in aqueous solution is reported for the first time. The theoretical analysis was carried out by using the cluster-continuum method recently proposed by us for calculating the free energy of solvation of ions. Unlike the gas-phase reaction, our results are consistent with the fact that the reaction occurs mainly by nucleophilic attack of the hydroxide on the carbonyl carbon to yield a tetrahedral intermediate ($B_{AC}2$ mechanism). However, an additional pathway, in which the hydroxide ion acts as a general base and a water molecule coordinated to this ion acts as the nucleophile, is also predicted to be important. The relative importance of

these pathways is calculated to be 87% and 13%, respectively. The tetrahedral intermediate of the hydrolysis reaction has an estimated lifetime of 10 nanoseconds, and its conjugate acid has a pK_a of 8.8. This tetrahedral intermediate is predicted to proceed to products by two pathways: elimination of methoxide ion (84%) and by water catalyzed elimination of methanol (16%). The less common reaction pathway, which involves attack of the hydroxide ion on the formyl hydrogen (decarbonylation mechanism) and leads to water, carbon

monoxide, and methanol, is calculated to be only 3 kcal mol⁻¹ less favorable than the $B_{AC}2$ mechanism. By comparison, direct attack of the hydroxide ion on the methyl group ($B_{AL}2$ or S_N2 mechanism) leading to an acyl-oxygen bond cleavage has a very high free energy of activation and is not expected to be important. The theoretically observed activation free energy at 298.15 K is calculated to be 15.5 kcal mol⁻¹, in excellent agreement with the experimentally measured value of 15.3 kcal mol⁻¹. This present model allows for a clear distinction between contributions due to solvation and those due to intrinsic (gas-phase) effects and proves to yield results in very good agreement with available experimental data.

Keywords: ab initio calculations • computer chemistry • ester hydrolysis • free-energy profile • nucleophilic addition

Introduction

Understanding the relationship between chemical reactivity and molecular structure has spearheaded much of modern chemical thinking. Yet, most of our knowledge in this area has been based on data obtained in condensed phases where the solvent can play an important role in dictating the energetics, the dynamics, and the outcome of chemical reactions. Thus, intrinsic chemical reactivity can often be obscured by solvent effects. These effects can become particularly relevant in reactions involving ionic species, in which strong electrostatic ion–solvent interactions may be present. This is well illustrated for S_N2 nucleophilic displacement reactions, in which nucleophiles with highly localized negative charges are known to react 10^{11} – 10^{15} times faster in the gas phase (solvent-free conditions) than in solution.^[1] On the experimental side, bridging the gap between intrinsic reactivity and reactivity in

solution ideally entails the characterization of chemical reactions under progressive stages of solvation. While some success has been achieved in studying the reactivity of gas-phase solvated ions,^[2] rate constants for these reactions become too slow to be measured by gas-phase techniques much before a solution-like environment can be monotonically attained. On the theoretical side, theoretical methods that explicitly incorporate solvent effects have, in recent years, provided an alternative and powerful approach toward relating solution behavior with intrinsic reactivity.^[3]

The hydrolysis of carboxylic esters in basic solution stands out as one of the most studied reactions in chemistry because of its common occurrence in many organic and biochemical processes. Yet dramatic differences are observed between intrinsic and solution reactivity. For simple esters, several important features characterize the gas-phase reaction: 1) unlike the reaction in solution,^[4] hydrolysis promoted by gas-phase OH^- ions proceeds competitively by both a $B_{AC}2$ mechanism (attack at the carbonyl center) and a B_{AL} or S_N2 mechanism (attack at the alkyl group of the ester);^[5] 2) for alkyl groups containing β -hydrogens, an $E2$ -type elimination mechanism can actually become the dominant mechanism for

[a] Prof. Dr. J. M. Riveros, Dr. J. R. Pliego, Jr.
Instituto de Química, Universidade de São Paulo
Caixa Postal 26077, CEP 05513-970 São Paulo, SP (Brazil)
Fax: (+55) 11-3818-3888
E-mail: josef@iq.usp.br, jmrnigra@quim.iq.usp.br

hydrolysis;^[5] 3) in formate esters an α -elimination process resulting in decarbonylation (the so-called Riveros reaction) is the most important reaction channel.^[6–8] The potential-energy surface for these gas-phase reactions is by now well understood as a result of recent calculations at increasingly higher levels of theory that are fully consistent with the observed experimental trends.^[9–12] Furthermore, these energy surfaces are particularly appropriate for analyzing gas-phase reactions within the realms of microcanonical transition-state theory, and application of simple statistical rate theories in the case of methyl formate has been shown to yield excellent agreement with the observed product distribution.^[12, 13]

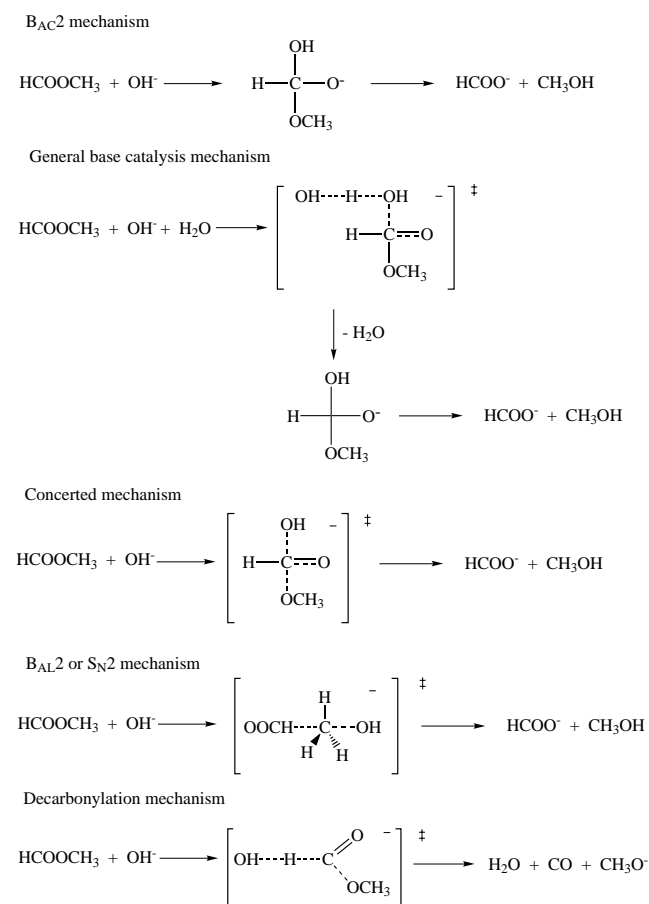
Over the years, many important and elucidative experimental studies have contributed to our understanding of the mechanistic features of ester hydrolysis in solution.^[14–20] Some of the classical mechanistic studies with labeled ^{18}O reagents established that the hydroxide ion reacts preferentially with esters of carboxylic acids by initial attack at the carbonyl center leading to the formation of a tetrahedral intermediate. This is then followed by loss of an alkoxide ion followed by rapid proton transfer to yield the carboxylate anion and the corresponding alcohol as products (see Scheme 1 for methyl formate).^[14, 15] More recently, Merlier^[18] has used heavy-atom isotope effects to conclude that formation of the tetrahedral intermediate is indeed largely rate-determining in the base hydrolysis of methyl formate. However, it has also been proposed that the attacking nucleophile in alkaline aqueous solution is actually water with general base assistance from

the hydroxide ion through a general base-catalysis mechanism. In this mechanism, a water molecule from the first coordination shell of the hydroxide ion is the true nucleophile and it is this water molecule that attacks the carbonyl center with loss of a proton to the hydroxide ion (Scheme 1). In addition, and based on kinetic studies, Stefanidis and Jencks^[19] have concluded that hydrolyses of formate esters are subject to general base catalysis by substituted acetate anions.

The mechanisms outlined above can change from stepwise to concerted for RCOOR' esters when the OR' group has a strong leaving group ability. In this case, the tetrahedral intermediate becomes a transition state;^[20] this leads to some general conclusions that can be summarized as follows:^[20] 1) for $\text{R}'\text{O}^-$ leaving groups with $\text{p}K_{\text{a}}$'s in the range $2 < \text{p}K_{\text{a}} < 11.7$, the reaction obeys a concerted mechanism; 2) for groups with $\text{p}K_{\text{a}}$'s > 11.7 , the reaction is stepwise with formation of the tetrahedral intermediate; 3) for groups with $\text{p}K_{\text{a}}$'s < 2 an acylium-ion-like intermediate should be formed. Other alternative mechanisms for ester hydrolysis have also been considered in solution. For example, attack at the alkyl group, the $\text{B}_{\text{AL}}2$ mechanism (essentially an $\text{S}_{\text{N}}2$ reaction) is extremely rare for carboxylic esters. Another uncommon mechanism proposed by Bruice and Holmquist^[17] for esters having hydrogens α to the carbonyl involves proton abstraction and formation of a carbanion with an enol-like structure. This species then yields the $\text{R}'\text{O}^-$ anion by elimination of a ketene, which then undergoes further reaction with water to generate the carboxylic acid product. Support for this mechanism comes from the observation that the reaction rate becomes independent of the hydroxide ion concentration above a certain pH. This kind of behavior was observed for esters of the type XCH_2COOAr ($\text{Ar} = o\text{-}$ or $p\text{-NO}_2\text{C}_6\text{H}_5$ and $\text{X} = \text{COOC}_2\text{H}_5$ or CN). Finally, formate esters can react with an hydroxide ion by still another pathway: a decarbonylation mechanism^[21] analogous to the gas-phase Riveros reaction. In this case, the hydroxide ion abstracts the formyl proton and promote the elimination of carbon monoxide to yield an alkoxide ion. Although this mechanism has not been reported for reactions in aqueous solution with hydroxide ion as the base, it does occur with *tert*-butoxide and hydride ions in aprotic solvents.

It is clear from the available experimental data summarized above that ester hydrolysis in basic solution can display a wide spectrum of mechanisms. Scheme 1 displays this variety of possible mechanisms for the base-induced hydrolysis of the simplest ester, that is, methyl formate. In this scheme, the carbanion mechanism described above has been excluded since this is not possible for formate esters.

The characterization of some of the mechanisms responsible for the basic hydrolysis of esters in aqueous solution by high-quality theoretical methods has only been explored recently. For example, Haeffner et al.^[22] have reported a study of the basic hydrolysis of methyl acetate at the MP2 level including the solvent by the PCM model. Both $\text{B}_{\text{AC}}2$ and $\text{S}_{\text{N}}2$ mechanisms were analyzed, and for the second step of the $\text{B}_{\text{AC}}2$ pathway two water molecules were explicitly included in the calculation. Their results point out that these explicit water molecules catalyze the methanol elimination step. In the meantime, Tantillo and Houk^[23] reported a theoretical



Scheme 1.

study of the basic hydrolysis of phenyl acetate at the MP2 level including the effect of the solvent through the PCM and SCI-PCM methods. Only the B_{AC}2 mechanism was explored and elimination of the phenoxide ion in the second step was found to proceed almost without a barrier. For *p*-nitrophenyl acetate, no barrier was found for the second step, in agreement with the view that the reaction in this case is a concerted process.

More recent theoretical work on the basic hydrolysis of methyl acetate and methyl formate in solution has been reported by Zhan et al.^[24, 25] A combination of a continuum model and inclusion of explicit water molecules was used to obtain theoretical values for the activation barriers of the B_{AC}2 and S_N2 mechanisms. The results agree with the general idea that the B_{AC}2 mechanism is the predominant one for these esters.^[25] Different pure continuum models were later applied to analyze the B_{AC}2 and S_N2 mechanisms for several alkyl esters.^[24] This approach has been further extended to theoretically characterize the energy barriers for alkaline ester hydrolysis of cocaine.^[26]

While the recent theoretical work on basic ester hydrolysis provides important information regarding the energetics of the reaction, not much attention has been given to the free-energy changes for the reaction in solution. Yet, *this is the most important thermodynamic parameter for analyzing solution reactions by transition-state theory*. Haeffner et al.^[22] did report their data as free energy, but the translational and rotational contributions were not included in the free-energy calculation. These effects *must* be included because they do make a very important contribution. On the other hand, Tantillo and Houk,^[23] and Zhan et al.^[24, 25] have only reported solution energies, that is, addition of the gas-phase energy to the free energy of solvation determined by the continuum model. Thus, a theoretical methodology is needed for establishing the free-energy profile of the reaction in solution if one is to make a meaningful comparison with the experimentally observed rate constants. Furthermore, the different mechanistic possibilities should be explored in order to understand the preferred reaction pathways and to bridge the important differences between gas-phase and solution reactivity.

As a follow up to our investigation of the gas-phase reaction between the hydroxide ion and methyl formate,^[12] the present report describes a full analysis of the free-energy profile of the possible pathways for the reaction in aqueous solution outlined in Scheme 1. Our analysis is based on a cluster-continuum method to calculate the free energy of solvation of ions, a hybrid approach recently proposed by us and tested for several organic ions.^[27, 28] We have shown this approach to be more stable than pure continuum models, and to yield good results for ionic species. In the first part of this paper, the details of the calculations are outlined, whereas in the second section we show how to apply the cluster-continuum model to chemical reactions. Comparison of our theoretical calculations with experimental results reveal excellent agreement for the kinetic parameters for the hydrolysis of methyl formate. Thus, these results suggest that this general methodology may prove to be of considerable value in detailing differences between gas-phase and solution reactivity.

Computational Methods

Ab initio calculations: The potential-energy surface for the reaction of solvated hydroxide ion with methyl formate was initially explored at the ab initio HF/6–31 + G(d,p) level of theory. Minima and transition-state structures were obtained by full geometry optimizations and characterized by harmonic frequency analysis. For these structures, single point calculations were then performed at higher levels of theory (namely MP2/6–311 + G(2df,2p) and MP4/6–31G)), in order to obtain more accurate energies. Finally, the additivity approximation^[29–33] was used to obtain effective MP4/6–311 + G(2df,2p) energies.

The bulk solvent effect was treated by the IPCM method^[34] by using the MP2/6–31 + G(d,p) wave function and an isodensity value of 0.0004. Statistical mechanics calculations were used to obtain the gas-phase thermodynamic parameters, and the free energy in aqueous solution was obtained by addition of the IPCM free energy of solvation to the gas-phase free energy. All calculations were done with the Gaussian 94 suite of programs.^[35]

The cluster-continuum model for chemical reactions: Several different theoretical protocols have been used in recent years to describe chemical reactions in aqueous solutions—particularly hydrolysis reactions of amides, sulfates, phosphates, and esters.^[3, 11, 26] The common approach, in which a molecule is represented by its gas-phase structure, and the free energy of solvation is calculated from a reaction field model is usually inadequate for ions in aqueous media and can lead to inaccurate results for the free energy of solvation of ions.^[27] This is due to the shortcomings of continuum models^[36] in properly accounting for strong electrostatic interactions and hydrogen bonding with some of the nearby neutral solvent molecules. This situation can be overcome in principle by addition of some explicit solvent molecules around the bare ion to form a cluster, or supermolecule, where specific solute–solvent interactions can be introduced in the theoretical model. This idea has been explored to describe solvation processes^[37–45] and it becomes an important consideration in the description of chemical reactions in the liquid phase, once an appropriate methodology is used to account for solvation. This type of approach has recently been proposed by us for calculating the free energy of solvation of ions.^[28] Our method, which we have labeled *the cluster-continuum model*, considers an ionic cluster as a distinct chemical species and optimizes the number of explicit solvent molecules in the cluster by searching for the most negative free energy of solvation resulting from the cluster interacting with the solvent, represented by a continuum model. This approach avoids the use of an a priori fixed number of explicit solvent molecules and can be extended to reaction and activation free energies in liquid solution as illustrated below.

Our model considers an ion A[±] (either a positive or negatively charged species) surrounded by *n* explicit solvent molecules, S, reacting with an organic molecule B to generate a product C[±] with its surrounding solvent molecules. The number *n* of solvent molecules around the A[±] ion is determined by the cluster-continuum method (see below) and the reaction can be formally written as:



Here *m* is the number of explicit solvent molecules released upon formation of the product ion and, for general purposes, it can be either a positive or negative integer. As A[±] and C[±] are different ions, the ideal number of solvent molecules that comply with the optimization for the lowest free energy of solvation is not necessarily the same. The next step is to determine the observed free energy of the reaction by using *T* = 298.15 K and 1 mol L^{−1} as the convention for our standard state (here represented by the superscript *) as shown in Equation (2):

$$\Delta G_R^* = \mu^*(C^{\pm}(S)_{n-m}) + m\mu^*(S) - \mu^*(A^{\pm}(S)_n) - \mu^*(B) \quad (2)$$

This leads to an equilibrium constant:

$$e^{-\Delta G^*/RT} = \frac{[C^{\pm}(S)_{n-m}][S]^m}{[A^{\pm}(S)_n][B]} \quad (3)$$

Here, the chemical potential of each species X in solution, μ^{*}(X), is the sum of the gas-phase chemical potential, μ_g^{*}(X), plus the free energy of solvation determined by the continuum IPCM model, ΔG_{solv}^{*}(X):

$$\mu^*(X) = \mu_g^*(X) + \Delta G_{solv}^*(X) \quad (4)$$

The observed equilibrium constant then takes the form:

$$e^{-\Delta G_{\text{obs}}^{\ddagger}/RT} = [S]^{-m} e^{\Delta G_R^{\ddagger}/RT} = \frac{[C^{\ddagger}](S)_{n-m}}{[A^{\ddagger}](S)_n[B]} = \frac{[C^{\ddagger}]}{[A^{\ddagger}][B]} \quad (5)$$

and the observed free energy takes the form:

$$\Delta G_{\text{obs}}^{\ddagger} = \Delta G_R^{\ddagger} + mRT \ln[S] \quad (6)$$

The number m of solvent molecules released in the reaction is then determined by the condition of the most negative reaction free energy. In other words, the number of explicit $n - m$ solvent molecules solvating the product C^{\ddagger} is varied in order to attain the most negative *observed reaction free energy* as defined by Equation (6). Thus, it is this property that must be compared with experimental free-energy data.

The same principle can be extended to transition states (TS) and can also be written as a formal equation:

$$A^{\ddagger}(S)_n + B \rightarrow TS^{\ddagger}(S)_{n-m} + mS \quad \Delta G^{*\ddagger} \quad (7)$$

The observed free energies of activation will then be:

$$\Delta G_{\text{obs}}^{*\ddagger} = \Delta G^{*\ddagger} + mRT \ln[S] \quad (8)$$

From this, rate constants can be calculated by the usual transition-state theory formula:

$$k(T) = \frac{k_b T}{h} e^{-\Delta G_{\text{obs}}^{*\ddagger}/RT} \quad (9)$$

Based on the above equations, free energies of reaction and activation were calculated for each reaction step of the $\text{OH}^- + \text{HCOOCH}_3$ system in aqueous solution. These results are given in the next sections.

Results and Discussion

Minima and transition-state structures: We have considered several possible reaction pathways, and the optimized structures are shown in Figures 1 and 2. Minima and transition-state structures are identified as **MS n x** and **TS n x**, respectively, where n refers to the step number in Scheme 2 and x indicates the number of solvent molecules around the corresponding structure ($b = 2$, $c = 3$ molecules).

The **TS1b** and **TS1c** transition states correspond to the nucleophilic attack of an hydroxide ion on the carbonyl center; this leads to the tetrahedral intermediate **MS1b** ($B_{AC}2$ mechanism). These structures reveal that the carbon(carbonyl)–oxygen(hydroxide) lengths in the transition states are predicted to be somewhat extended C–O bonds, namely 1.90 Å and 1.82 Å. Another transition state leading to the tetrahedral intermediate is the **TS2c** structure, which corresponds to a general base-catalysis mechanism by the hydroxide ion. In this mechanism, it is noticeable that the attacking nucleophile is one of the water molecules solvating the OH^- ion. It is this molecule that donates the proton to the hydroxide ion while the carbon–oxygen bond is being formed.

The **TS3b** structure corresponds to a S_N2 mechanism, in which the hydroxide ion attacks the methyl group to yield methanol and the formate ion in a single step. The last possibility considers attack of the hydroxide ion on the formyl hydrogen to abstract a proton with simultaneous formation of carbon monoxide and methoxide ion (structure **TS4b**). This pathway has been defined as the decarbonylation mechanism.

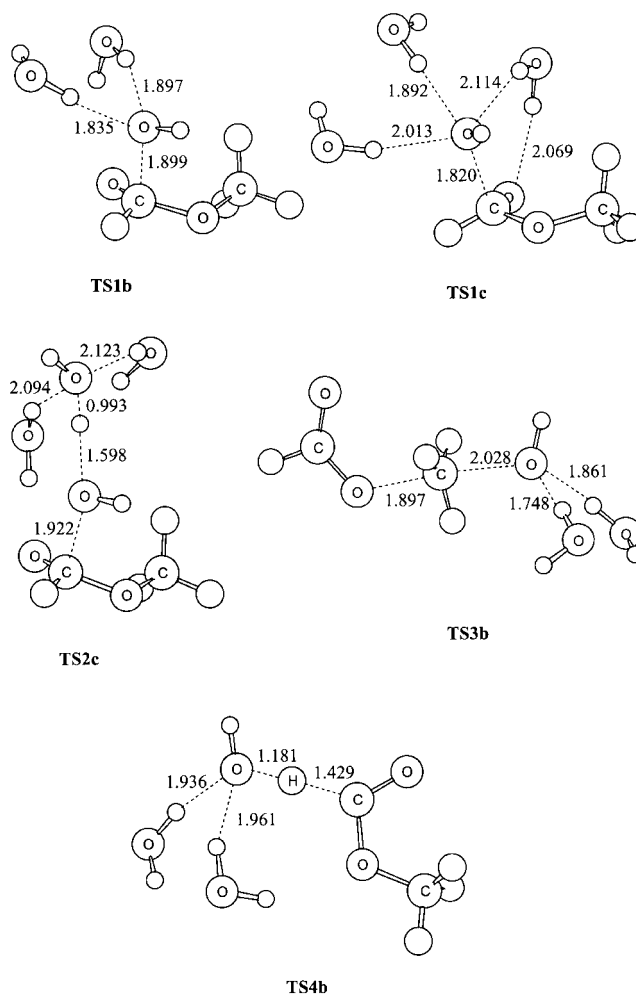


Figure 1. Transition-state structures for the first steps of the reaction $\text{OH}^- + \text{HCOOCH}_3$ in aqueous solution (see Scheme 2).

The tetrahedral intermediate formed in steps 1 and 2 can proceed to products by three pathways. The first possibility is direct elimination of methanol via **TS5b**. This elimination can also be catalyzed by one water molecule, leading to structure **TS6b**. The third pathway is elimination of a methoxide ion with formation of formic acid (**TS7b**) followed by proton abstraction by the methoxide ion. An additional alternative would be formation of the protonated tetrahedral intermediate, **MS4**; this intermediate has also been considered in order to evaluate the possibility of this route.

Free-energy profile: Calculated activation and reaction thermodynamic parameters for the different pathways of the reaction between the solvated hydroxide ion cluster and methyl formate are listed in Tables 1 and 2. The number of water molecules around the hydroxide ion was varied in the calculations to search for the “ideal” number of solvent molecules that leads to a free-energy minimum. Steps are again numbered according to Scheme 2 and the number of explicit solvent molecules included are identified as $b = 2$, $c = 3$ water molecules. For example, step 1 corresponds to the nucleophilic attack of the hydroxide ion on the carbonyl group of the methyl formate. In process 1b, two water

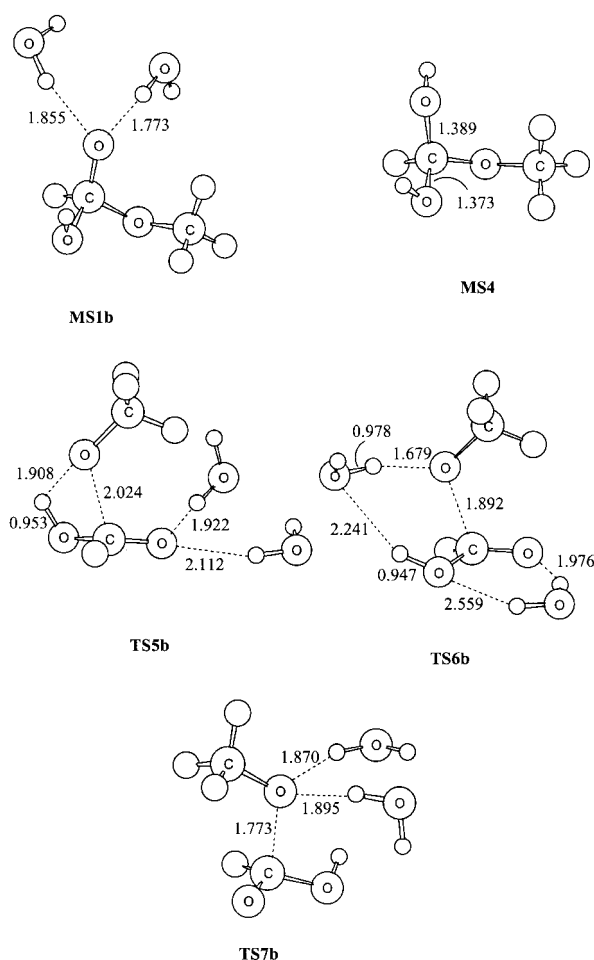
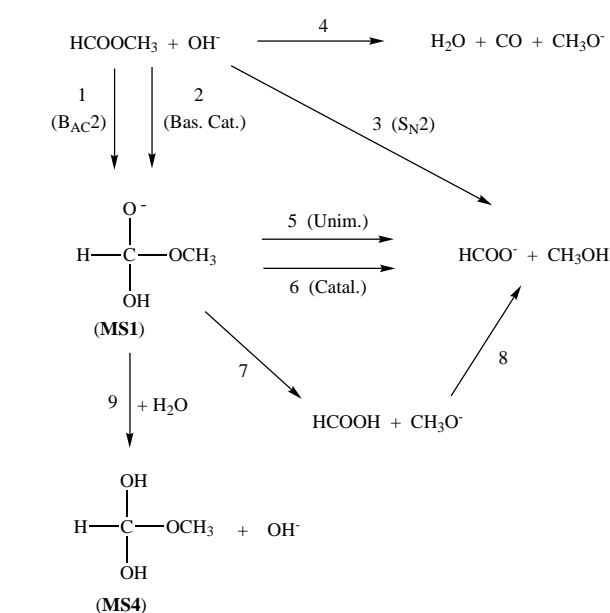


Figure 2. Minima and transition-state structures for the decomposition of the tetrahedral intermediate formed in the reaction $\text{OH}^- + \text{HCCOCH}_3$ (see Scheme 2).

molecules are maintained in the transition state while one water is released as a free solvent molecule. In process 1c, all water molecules are included in the explicit solvation of the transition state.



Scheme 2.

Based on the data in Tables 1 and 2, activation and reaction free energies for the $\text{OH}^- + \text{HCOOCH}_3$ reaction system in aqueous solution can be predicted theoretically by using the equations described above. This can be exemplified by considering process 1b: the activation free energy, ΔG^{\ddagger} in Equation (7), is calculated to be $13.31 \text{ kcal mol}^{-1}$ but this value must be corrected by $2.38 \text{ kcal mol}^{-1}$ according to Equation (8) in order to correlate the free energies given by our cluster-continuum model with the experimental (or observed) values. This procedure yields $15.69 \text{ kcal mol}^{-1}$ for what we have labeled the observed free energy of activation, $\Delta G_{\text{obs}}^{\ddagger}$, according to Equation (8). The same approach for process 1c, in which all three molecules of water are retained in the transition-state cluster, yields an activation free energy, $\Delta G_{\text{obs}}^{\ddagger}$, of $15.15 \text{ kcal mol}^{-1}$. Thus, according to the free-energy minimum criterion of our model, three is the ideal number of solvent molecules solvating the transition state, and we take

Table 1. Calculated activation parameters for different pathways of the $\text{HCOOCH}_3 + \text{OH}^-(\text{H}_2\text{O})_3$ reaction.^[a]

	1b	1c	2c	3b	4b	4c	5b	6b	7b
E [MP2/6–31G]	9.31	−9.29	−7.43	18.63	12.77	−3.80	13.55	4.10	2.69
E [MP2/6–31 + G(d,p)]	10.60	−3.31	−2.18	26.27	16.48	4.00	17.56	10.13	7.34
E [MP2/6–311 + G(2df,2p)]	10.45	−3.08	−1.57	26.74	16.24	4.31	17.34	10.09	7.69
E [MP4/6–31G]	7.46	−11.41	−8.96	16.39	11.44	−5.34	12.83	3.97	2.43
E [MP4/6–311 + G(2df,2p)] ^[b]	8.59	−5.19	−3.10	24.50	14.91	2.77	16.62	9.96	7.43
ΔZPE^{\ddagger} ^[c]	−0.40	2.32	2.09	−2.47	−4.53	−2.03	−2.77	−1.94	−1.15
ΔE^{\ddagger} ^[d]	8.19	−2.88	−1.01	22.04	10.38	0.74	13.85	8.03	6.28
ΔH_g^{\ddagger}	8.36	−2.90	−1.24	22.85	10.84	1.29	14.35	8.15	6.10
ΔS_g^{\ddagger}	−13.34	−36.59	−37.75	−4.60	−10.12	−30.92	5.43	1.15	−3.73
ΔG_g^{\ddagger}	12.34	8.01	10.01	24.23	13.86	10.51	12.73	7.81	7.21
$\Delta \Delta G_{\text{sol}}^{\ddagger}$ ^[e]	0.98	7.15	6.28	4.74	1.90	9.94	2.79	0.27	−0.11
$\Delta G_{\text{sol}}^{\ddagger}$	13.31	15.15	16.29	28.97	15.77	20.45	15.52	8.08	7.11

[a] Units of kcal mol^{-1} except for the entropy ($\text{cal K}^{-1} \text{mol}^{-1}$). Standard state defined for $T = 298.15 \text{ K}$ and 1 mol L^{-1} for all species. The numbers correspond to the following processes (see also text for the nomenclature, b = two, c = three explicit solvent molecules): 1b) $\text{HCOOCH}_3 + \text{OH}^-(\text{H}_2\text{O})_3 \rightarrow \text{TS1b} + \text{H}_2\text{O}$, 1c) $\text{HCOOCH}_3 + \text{OH}^-(\text{H}_2\text{O})_3 \rightarrow \text{TS1c}$, 2c) $\text{HCOOCH}_3 + \text{OH}^-(\text{H}_2\text{O})_3 \rightarrow \text{TS2c}$, 3b) $\text{HCOOCH}_3 + \text{OH}^-(\text{H}_2\text{O})_3 \rightarrow \text{TS3b} + \text{H}_2\text{O}$, 4b) $\text{HCOOCH}_3 + \text{OH}^-(\text{H}_2\text{O})_3 \rightarrow \text{TS4b} + \text{H}_2\text{O}$, 4c) $\text{HCOOCH}_3 + \text{OH}^-(\text{H}_2\text{O})_3 \rightarrow \text{TS4c}$, 5b) $\text{MS1b} \rightarrow \text{TS5b}$, 6b) $\text{MS1b} \rightarrow \text{TS6b}$, 7b) $\text{MS1b} \rightarrow \text{TS7b}$. [b] Obtained by additivity approximation. [c] Variation of zero-point vibrational energy obtained at the HF/6–31 + G(d,p) level. [d] Activation energy at the MP4/6–311 + G(2df,2p) level plus ΔZPE . [e] Variation of free energy of solvation (in going from the gas-phase to solution) obtained by using the IPCM method with the MP2/6–31 + G(d,p) wave function. Dielectric constant of 78.0 and isodensity value of 0.0004.

Table 2. Calculated reaction parameters for different pathways of the $\text{HCOOCH}_3 + \text{OH}^-(\text{H}_2\text{O})_3$ reaction (see Scheme 2).^[a]

	1b	1c	3b	4c	7c	8b	9c
E [MP2/6-31G]	4.62	-17.41	-7.55	7.00	-4.78	-7.39	2.45
E [MP2/6-31+G(d,p)]	2.46	-13.66	-5.70	12.09	1.05	-9.22	1.59
E [MP2/6-311+G(2df,2p)]	1.57	-13.84	-6.48	12.89	1.37	-9.42	2.37
E [MP4/6-31G]	2.92	-19.26	-8.67	5.97	-3.70	-7.89	3.44
E [MP4/6-311+G(2df,2p)] ^[b]	-0.13	-15.70	-7.60	11.86	2.45	-9.93	3.36
ΔZPE ^[c]	0.96	4.10	-2.43	-5.26	-1.04	-2.35	3.33
ΔE ^[d]	0.83	-11.60	-10.03	6.60	1.42	-12.27	6.69
ΔH_g	0.84	-11.73	-9.42	8.08	1.57	-11.83	5.96
ΔS_g	-14.08	-36.94	23.30	25.27	14.65	22.73	-13.45
ΔG_g	5.04	-0.72	-16.37	0.55	-2.80	-18.61	9.97
$\Delta\Delta G_{\text{solv}}$ ^[e]	0.72	10.07	-2.83	1.03	1.56	-5.12	1.86
ΔG_{sol}	5.76	9.35	-19.20	1.58	-1.24	-23.73	11.82

[a] Units of kcal mol^{-1} except for the entropy ($\text{cal K}^{-1} \text{mol}^{-1}$). Standard state defined for $T=298.15 \text{ K}$ and 1 mol L^{-1} for all species. The numbers correspond to the following processes (see also text for the nomenclature, b=two, c=three explicit solvent molecules): 1b) $\text{HCOOCH}_3 + \text{OH}^-(\text{H}_2\text{O})_3 \rightarrow \text{MS1b} + \text{H}_2\text{O}$, 1c) $\text{HCOOCH}_3 + \text{OH}^-(\text{H}_2\text{O})_3 \rightarrow \text{MS1c}$, 3b) $\text{HCOOCH}_3 + \text{OH}^-(\text{H}_2\text{O})_3 \rightarrow \text{HCOO}^-(\text{H}_2\text{O})_2 + \text{CH}_3\text{OH} + \text{H}_2\text{O}$, 4c) $\text{HCOOCH}_3 + \text{OH}^-(\text{H}_2\text{O})_3 \rightarrow \text{CH}_3\text{O}^-(\text{H}_2\text{O})_3 + \text{CO} + \text{H}_2\text{O}$, 7c) $\text{MS1b} + \text{H}_2\text{O} \rightarrow \text{CH}_3\text{O}^-(\text{H}_2\text{O})_3 + \text{HCOOH}$, 8b) $\text{CH}_3\text{O}^-(\text{H}_2\text{O})_3 + \text{HCOOH} \rightarrow \text{HCOO}^-(\text{H}_2\text{O})_2 + \text{CH}_3\text{OH} + \text{H}_2\text{O}$, 9c) $\text{MS1b} + 2\text{H}_2\text{O} \rightarrow \text{MS4} + \text{OH}^-(\text{H}_2\text{O})_3$. [b] Obtained by additivity approximation. [c] Variation of zero point vibrational energy obtained at the HF/6-31+G(d,p) level. [d] Reaction energy at the MP4/6-311+G(2df,2p) level plus ΔZPE . [e] Variation of free energy of solvation (in going from the gas-phase to solution) obtained using the IPCM method with the MP2/6-31+G(d,p) wave function. Dielectric constant of 78.0 and isodensity value of 0.0004.

15.15 kcal mol^{-1} as the activation free energy for step 1. By extending this procedure to all the steps in Scheme 2, we obtained our best values for the reaction and activation free energies for the $\text{OH}^- + \text{HCOOCH}_3$ system in aqueous solution and these are displayed in Table 3. This table contains all the necessary information to build the free-energy profile of the aqueous solution reaction that is shown in Figure 3.

A close analysis of Figure 3 enables us to predict the most likely reaction mechanisms, products, reaction kinetics, and

Table 3. Activation and reaction free energies for steps 1 to 9 in the $\text{OH}^- + \text{HCOOCH}_3$ system in aqueous solution calculated by the cluster-continuum model.^[a]

Reaction step	ΔG^{**}	ΔG^*
1	15.15	8.14
2	16.29	8.14
3	31.35	-16.82
4	18.15	1.58
5	15.52	-24.96
6	8.08	-24.96
7	7.11	-3.62
8	-	-21.35
9	-	9.44

[a] The free energies contained in this table (in kcal mol^{-1}) refer to the observed values as calculated from equation 8 (see text). Standard state defined for $T=298.15 \text{ K}$ and 1 mol L^{-1} for all species. The numbers correspond to the processes shown in Scheme 2.

equilibrium constants. It is clear that step 1, corresponding to the $\text{B}_{\text{AC}2}$ mechanism, has the lowest activation free energy (15.2 kcal mol^{-1}) for the first reaction step. However, it should be noted that the general basis catalysis mechanism (step 2) is also characterized by a comparatively low free energy of activation, $\Delta G^{**}=16.3 \text{ kcal mol}^{-1}$. Thus, both mechanisms are expected to contribute to the first reaction step. By comparison, the $\text{S}_{\text{N}2}$ mechanism is characterized by a very unfavorable activation free energy of 31.4 kcal mol^{-1} , and would not be expected to contribute to the overall reaction. Surprisingly enough, the decarbonylation mechanism, step 4, is predicted to have $\Delta G^{**}=18.2 \text{ kcal mol}^{-1}$. While this value

is above that of pathways 1 and 2, it is still within the range that deserves further consideration, even though the products are 1.6 kcal mol^{-1} higher than the reactants. Based on this relatively low activation free energy, the decarbonylation mechanism would be predicted to account for about 1 % of the overall $\text{OH}^- + \text{HCOOCH}_3$ reaction in aqueous solution.

The stable tetrahedral intermediate of the hydrolysis reaction, **MS1**, formed by step 1 or 2 is predicted by our calculations to lie 8.1 kcal mol^{-1} above the reactants in this free energy profile. The tetrahedral intermediate can proceed to the formate anion plus methanol as final products by three pathways, or undergo protonation to yield **MS4**. The three pathways for the tetrahedral intermediate are: a) unimolecular elimination of methanol (step 5) for which ΔG^{**} is calculated to be 15.5 kcal mol^{-1} ; b) catalytic elimination of methanol (step 6) for which ΔG^{**} is predicted to be 8.1 kcal mol^{-1} ; and c) direct elimination of methoxide ion followed by proton transfer (step 7) for which the calculations yield a ΔG^{**} of 7.1 kcal mol^{-1} . The final $\text{HCOO}^- + \text{CH}_3\text{OH}$ products are 16.8 kcal mol^{-1} below the initial reactants in this free-energy profile. By comparison, the protonated tetrahedral intermediate (**MS4**) is located 17.6 kcal mol^{-1} above the free energy of the reagents. These results indicate that the decomposition step of the tetrahedral intermediate should occur primarily through **TS7b** with a minor contribution from process 6 and its transition state **TS6b**. In addition, based on process 9c in Table 2, we can predict the pK_{a} of the protonated tetrahedral intermediate to be in the range of 8.8. Thus, the tetrahedral intermediate is not expected to be protonated in alkaline solution.

Our analysis of the $\text{OH}^- + \text{HCOOCH}_3$ reaction in aqueous solution clearly agrees with the notion that the $\text{B}_{\text{AC}2}$ mechanism should be the dominant pathway for methyl formate. However, some contribution is expected from the general basic-catalysis mechanism. Furthermore, decomposition of the tetrahedral intermediate is expected to occur mainly by elimination of a methoxide ion, and to a lesser extent by catalytic elimination of methanol. Finally, the decarbonylation mechanism is predicted to be only 3 kcal mol^{-1} less

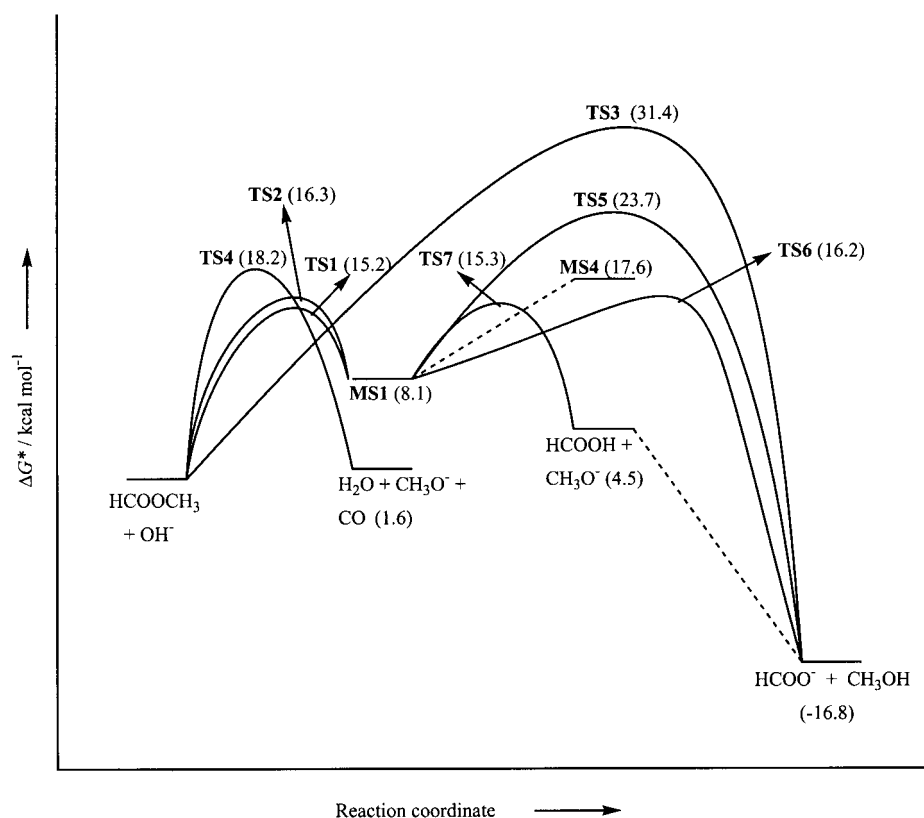


Figure 3. Calculated free-energy profile for the reaction $\text{OH}^- + \text{HCOOCH}_3$. The steps are numbered according to Scheme 2.

favorable than the $\text{B}_{\text{AC}}2$ mechanism, while the $\text{S}_{\text{N}}2$ mechanism is very unfavorable and should not be observed.

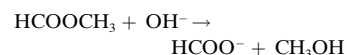
Comparison with experimental data: While the general picture derived from our calculations agrees well with what is known about the methyl formate reaction, a more quantitative comparison with experiment is necessary for a proper evaluation of our methodology.

In our original proposal of the cluster-continuum model, the general approach was shown to be very stable and to yield a uniform treatment of solvation for different ions. Comparison of our present calculations with available experimental thermodynamic and kinetic data can then contribute to assessing the reliability of our results. Compilation of thermodynamic data presently available can be used to obtain the reaction free energies for the hydrolysis and decarbonylation reactions, while kinetic data has been used to extract the observed activation free energy.

Table 4 lists the enthalpy of formation of the relevant species taken from the literature.^[46, 47] The gas-phase entropy can be obtained with high accuracy by use of theoretical

methods, and the results of our ab initio calculations were used to determine this property. Finally, experimental values for solvation free energies were taken from our recent paper.^[27] These data were combined to determine the gas-phase and aqueous solution reaction free energies for the hydrolysis and the decarbonylation reactions, and are indicated in Table 5.

The hydrolysis reaction:



has an experimental reaction free energy of solution (ΔG_{sol}^*) of $-13.0 \text{ kcal mol}^{-1}$, while the theoretical value calculated by our model amounts to $-16.8 \text{ kcal mol}^{-1}$. While this is reasonably good agreement, it is interesting to explore how much of this free energy is due to the gas-phase contribution (ΔG_{g}^*) and how much to the aqueous solution contribution

($\Delta\Delta G_{\text{sol}}^*$) due to the solvation of neutrals and ionic species. The experimental ΔG_{g}^* is $-41.1 \text{ kcal mol}^{-1}$, which is comparable with the theoretical value of $-43.9 \text{ kcal mol}^{-1}$. On the other hand, the experimental and theoretical aqueous solution contributions are $28.1 \text{ kcal mol}^{-1}$ and $27.1 \text{ kcal mol}^{-1}$,

Table 4. Experimental and theoretical gas-phase thermodynamic parameters and experimental free energy of solvation for reactants and products.

Species	ΔH_{f}^0 ^[a]	ΔS_{g}^0 ^[b]	ΔG_{sol}^* ^[c]
H_2O	-57.80	45.1	-6.3
CO	-26.42	47.3	1.18 ^[d]
CH_3OH	-48.07	56.8	-5.10
HCOOCH_3	-86.6	67.6	-2.78 ^e
OH^-	-32.8	41.2	-105.0
CH_3O^-	-32.2	52.8	-94.0
HCOO^-	-110.9	57.1	-74.6

[a] Gas-phase enthalpy of formation (in kcal mol^{-1}) at 298.15 K taken from ref. [45]. [b] Gas-phase entropy (in $\text{cal K}^{-1} \text{ mol}^{-1}$) at 1 atm and 298.15 K calculated by statistical mechanics with our MP2/6-31+G(d) ab initio data (molecular structure and vibrational frequencies). [c] Experimental free energy of solvation (in kcal mol^{-1}) taken from ref. [27]. Standard state of 1 mol L^{-1} . [d] Obtained by theoretical calculation at the SM5.42R/HF/6-31G* level. [e] See ref. [46].

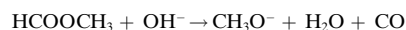
Table 5. Thermodynamic parameters for the gas-phase and aqueous solution reaction.^[a]

Reaction	ΔG_{g}^*	Experimental ^[b] $\Delta\Delta G_{\text{sol}}^*$	ΔG_{sol}^*	ΔG_{g}^*	Theoretical ^[c] $\Delta\Delta G_{\text{sol}}^*$	ΔG_{sol}^*
$\text{HCOOCH}_3 + \text{OH}^- \rightarrow \text{HCOO}^- + \text{CH}_3\text{OH}$	-41.1	28.1	-13.0	-43.9	27.1	-16.8
$\text{HCOOCH}_3 + \text{OH}^- \rightarrow \text{CH}_3\text{O}^- + \text{H}_2\text{O} + \text{CO}$	-5.9	8.7	2.8	-6.2	7.8	1.6

[a] Standard state of 1 mol L^{-1} for all species, $T = 298.15 \text{ K}$; units of kcal mol^{-1} . [b] Values obtained from Table 4. [c] Solvent effect calculated by the cluster-continuum model.

respectively. Thus, the main contribution to the difference between experiment and theory ($2.8 \text{ kcal mol}^{-1}$) arises from the gas-phase values, whereas the solution contribution due to solvation (according to the cluster-continuum method) amounts only to 1 kcal mol^{-1} . This difference is well within the experimental uncertainty ($\pm 2 \text{ kcal mol}^{-1}$) of the enthalpy of formation of the HCOO^- ion.

For the decarbonylation reaction:



excellent agreement is observed between the experimental value of $2.8 \text{ kcal mol}^{-1}$ for ΔG_{sol}^* and the theoretically calculated value of $1.6 \text{ kcal mol}^{-1}$. The corresponding experimental and theoretical gas-phase contributions (ΔG_{g}^*) are $-5.9 \text{ kcal mol}^{-1}$ and $-6.2 \text{ kcal mol}^{-1}$, respectively, while the experimental and theoretical solution-phase contributions ($\Delta \Delta G_{\text{sol}}^*$) are $8.7 \text{ kcal mol}^{-1}$ and $7.8 \text{ kcal mol}^{-1}$, respectively. Again, the cluster-continuum model provides excellent quantitative prediction of the solvent effect.

Yet, the most important test to assess the methodology used to describe these reactions in aqueous solution is to verify its ability to predict the activation free energy of the reaction. The overall rate constant for the reaction of the hydroxide ion with methyl formate in aqueous solution was determined many years ago, by Humphreys and Hammett,^[16] to be $38.4 \text{ L mol}^{-1} \text{ s}^{-1}$ at 298.15 K , and corresponds to $\Delta G_{\text{sol}}^{*+} = 15.3 \text{ kcal mol}^{-1}$. Considering both the $\text{B}_{\text{AC}}2$ and the general base-catalysis mechanisms to be operating in the overall reaction, and assuming that the tetrahedral intermediate (**MS1**) proceeds to products through steps 6 and 7, we can use Scheme 3 and the stationary state approximation to derive the theoretical observed rate constant as:

$$k_{\text{obs}} = \frac{(k_1 + k_2)(k_6 + k_7)}{(k_{-1} + k_{-2}) + (k_6 + k_7)} \quad (10)$$

The individual rate constants can be obtained from the data in Table 3 by using transition-state theory, and amount to:

$$k_1 = 4.9 \times 10^1 \text{ L mol}^{-1} \text{ s}^{-1} \quad k_2 = 7.1 \text{ L mol}^{-1} \text{ s}^{-1}$$

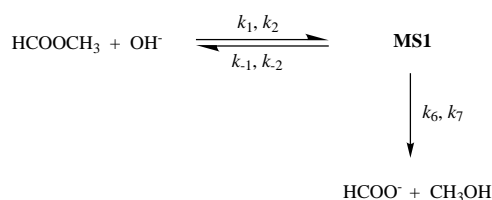
$$k_{-1} = 4.5 \times 10^7 \text{ s}^{-1} \quad k_{-2} = 6.6 \times 10^6 \text{ s}^{-1}$$

$$k_6 = 7.4 \times 10^6 \text{ s}^{-1} \quad k_7 = 3.8 \times 10^7 \text{ s}^{-1}$$

This yields a theoretical observed rate constant of:

$$k_{\text{obs}} = 26 \text{ L mol}^{-1} \text{ s}^{-1}$$

and $\Delta G_{\text{sol}}^{*+} = 15.5 \text{ kcal mol}^{-1}$. This theoretical value for the free energy of activation is in excellent agreement with the experimental value of $15.3 \text{ kcal mol}^{-1}$. It is therefore possible to conclude that our cluster-continuum method is able to predict very accurately the activation free energy for the basic hydrolysis of methyl formate in aqueous solution.



Scheme 3.

Conclusion

The results of the present theoretical study are consistent with the experimental evidence that the basic hydrolysis of alkyl esters in aqueous solution proceeds primarily by the $\text{B}_{\text{AC}}2$ mechanism. Unlike the analogous gas-phase reaction of OH^- with HCOOCH_3 previously characterized^[11, 12] solvation has two major effects: a) it stabilizes the hydroxide ion dramatically compared with the tetrahedral intermediate; this leads to a sizable activation free energy for the reaction; b) whereas the hydrolysis reaction in the gas phase is initiated by formation of an ion-dipole $\text{S}_{\text{N}}2$ type complex,^[48] $[\text{HO}^- \cdots \text{H}_3\text{COOCH}]$, which either rearranges to the tetrahedral intermediate or proceeds to products by an $\text{S}_{\text{N}}2$ mechanism,^[12] the transition state for this mechanism is poorly solvated when compared with the $\text{B}_{\text{AC}}2$ pathway and solvation is responsible for making the $\text{S}_{\text{N}}2$ reaction highly unfavorable.

A second important consideration that emerges from our results is the importance of a general base-catalysis mechanism. We have found that, while the first reaction step (see Scheme 2) corresponds to a nucleophilic attack of the hydroxide ion to the carbonyl carbon (the main reaction pathway), a measurable part of the reaction proceeds by a general basic-catalysis mechanism, in which a water molecule in the first coordination shell of the hydroxide ion acts as the nucleophile. This pathway is predicted to account for approximately 13% of the first step. The resulting tetrahedral intermediate has an expected short lifetime ($\approx 10 \text{ ns}$) and is predicted to decompose to products by two pathways: by direct elimination of methoxide ion or by water-catalyzed elimination of methanol in a 84% to 16% ratio.

Another interesting result is the decarbonylation mechanism, in which the hydroxide ion attacks the formyl hydrogen to give water, carbon monoxide, and methanol. While this is the preferred pathway in the gas phase, in which relative acidities are considerably different from those in aqueous solution, we find the activation free energy for this pathway to be only 3 kcal mol^{-1} less favorable than the free-energy barrier for the $\text{B}_{\text{AC}}2$ mechanism. Thus, we are led to speculate that this pathway could become a dominant feature of the reaction in aprotic low-polarity solvents. The fact that the decarbonylation mechanism has been observed in the reaction of *tert*-butoxide ion with formate esters in polar aprotic solvents^[21] supports this contention.

Overall, the experimental kinetic and thermodynamic data are in excellent agreement with our theoretical results. This observation is very rewarding and encouraging for the method introduced in this paper and is highly indicative of the quality of results that can be obtained by the cluster-continuum

method. It is well known that accurate modeling of ionic reactions in the liquid phase is a hard task, and the development of practical and reliable methods capable of handling these systems is timely. We hope that extension of these results to other ion-neutral reactions in the liquid phase may prove valuable in two ways: 1) to provide a convenient methodology for understanding how solvation can change intrinsic reactivity, and 2) to establish that a combination of continuum models with inclusion of some explicit solvent molecules is probably an accurate and yet relatively practical approach for the theoretical modeling of chemical reactions in the liquid phase at the present time.

Acknowledgements

The authors wish to thank the São Paulo Science Foundation for a postdoctoral fellowship (J.R.P.) and for continuous support of our research program. One of us (J.M.R.) also acknowledges support of the Brazilian Research Council (CNPq) through its Senior Research Fellowship program.

- [1] See for example: a) J. M. Riveros, S. M. José, K. Takashima, *Adv. Phys. Org. Chem.* **1985**, 21, 197; b) C. H. DePuy, S. Gronert, A. Mullin, V. M. Bierbaum, *J. Am. Chem. Soc.* **1990**, 112, 8650; c) S. Gronert, *Chem. Rev.* **2001**, 101, 329, and references therein.
- [2] See for example: a) D. K. Bohme, G. I. Mackay, *J. Am. Chem. Soc.* **1981**, 103, 978; b) D. K. Bohme, A. B. Raksit, *J. Am. Chem. Soc.* **1984**, 106, 3447; c) R. A. J. O'Hair, G. E. Davico, J. Hacaloglu, T. T. Dang, C. H. DePuy, V. M. Bierbaum, *J. Am. Chem. Soc.* **1994**, 116, 3609; d) P. M. Hierl, A. F. Ahrens, M. Henchman, A. A. Viggiano, J. F. Paulson, D. C. Clary, *J. Am. Chem. Soc.* **1986**, 108, 3142; e) A. A. Viggiano, S. T. Arnold, R. A. Morris, A. F. Ahrens, P. M. Hierl, *J. Phys. Chem.* **1996**, 100, 14397; f) S. T. Arnold, A. A. Viggiano, *J. Phys. Chem. A* **1997**, 101, 2859; g) H. Wincel, E. Mereand, A. W. Castleman, Jr., *J. Phys. Chem.* **1996**, 100, 7488; h) H. Wincel, E. Mereand, A. W. Castleman, Jr., *J. Phys. Chem. A* **1997**, 101, 8248; i) X. Yang, A. W. Castleman, Jr., *J. Am. Chem. Soc.* **1991**, 113, 6766; j) X. Yang, A. W. Castleman, Jr., *J. Phys. Chem.* **1991**, 95, 6182; k) U. Achatz, S. Joos, C. Berg, T. Schindler, M. Beyer, G. Albert, G. Niedner-Schatteburg, V. E. Bondybey, *J. Am. Chem. Soc.* **1998**, 120, 1876.
- [3] For some recent theoretical modeling of reactions of in water solution, see: a) B. Ensing, E. J. Meijer, P. E. Blöchl, E. J. Baerends, *J. Phys. Chem. A* **2001**, 105, 3300; b) X. Lopez, A. Dejaegere, M. Karplus, *J. Am. Chem. Soc.* **1999**, 121, 5548; c) D. Bakowies, P. A. Kollman, *J. Am. Chem. Soc.* **1999**, 121, 5712; d) J. Florián, A. Warshel, *J. Phys. Chem. B* **1998**, 102, 719; e) C. Amovilli, F. M. Floris, M. Sola, J. Tomasi, *Organometallics* **2001**, 20, 1310.
- [4] The prevalent mechanism of base-induced hydrolysis is discussed at length in textbooks such as: a) F. A. Carey, R. J. Sundberg, *Advanced Organic Chemistry, Part A: Structure and Mechanisms*, 3rd ed. Plenum, New York, **1990**, p. 465; b) T. H. Lowry, K. S. Richardson, *Mechanism and Theory in Organic Chemistry*, 2nd ed. Harper & Row, New York, **1981**, p. 650.
- [5] K. Takashima, J. M. Riveros, *J. Am. Chem. Soc.* **1978**, 100, 6128.
- [6] J. F. G. Faigle, P. C. Isolani, J. M. Riveros, *J. Am. Chem. Soc.* **1976**, 98, 2049.
- [7] C. H. DePuy, J. J. Grabowski, V. M. Bierbaum, S. Ingemann, N. M. M. Nibbering, *J. Am. Chem. Soc.* **1985**, 107, 1093.
- [8] B. T. Frink, C. M. Hadad, *J. Chem. Soc. Perkin Trans. 2* **1999**, 2397.
- [9] W. L. Jorgensen, J. F. Blake, J. D. Madura, S. G. Wierschke, *ACS Symp. Ser.* **1987**, 353, 200.
- [10] J. Pranata, *J. Phys. Chem.* **1994**, 98, 1180.
- [11] C.-G. Zhan, D. W. Landry, R. L. Ornstein, *J. Am. Chem. Soc.* **2000**, 122, 1522.
- [12] J. R. Pliego, Jr., J. M. Riveros, *Chem. Eur. J.* **2001**, 7, 169.
- [13] J. R. Pliego, Jr., J. M. Riveros, *J. Phys. Chem. A* **2002**, 106, 371.
- [14] a) M. L. Bender, R. S. Dewey, *J. Am. Chem. Soc.* **1956**, 78, 317; b) M. L. Bender, R. D. Ginger, J. P. Unik, *J. Am. Chem. Soc.* **1958**, 80, 1044; c) S. A. Shain, J. F. Kirsch, *J. Am. Chem. Soc.* **1968**, 90, 5848.
- [15] a) M. L. Bender, *Chem. Rev.* **1960**, 60, 53; b) S. L. Johnson, *Adv. Phys. Org. Chem.* **1967**, 5, 237.
- [16] H. M. Humphreys, L. P. Hammett, *J. Am. Chem. Soc.* **1956**, 78, 521.
- [17] T. C. Bruice, B. Holmquist, *J. Am. Chem. Soc.* **1968**, 90, 7136.
- [18] J. F. Marlier, *J. Am. Chem. Soc.* **1993**, 115, 5935.
- [19] D. Stefanidis, W. P. Jencks, *J. Am. Chem. Soc.* **1993**, 115, 6045.
- [20] a) S. Ba-Saif, A. K. Luthra, A. Williams, *J. Am. Chem. Soc.* **1989**, 111, 2647; b) J. P. Guthrie, *J. Am. Chem. Soc.* **1991**, 113, 3941; c) A. C. Hengge, R. A. Hess, *J. Am. Chem. Soc.* **1994**, 116, 11256; d) M. A. Fernandez, R. H. de Rossi, *J. Org. Chem.* **1999**, 64, 6000; e) A. Williams, *Acc. Chem. Res.* **1989**, 22, 387.
- [21] J. C. Powers, R. Seidner, T. G. Parsons, *Tetrahedron Lett.* **1965**, 1713.
- [22] F. Haeflner, C.-H. Hu, T. Brinck, T. Norin, *THEOCHEM* **1999**, 459, 85.
- [23] D. J. Tantillo, K. N. Houk, *J. Org. Chem.* **1999**, 64, 3066.
- [24] C.-G. Zhan, D. W. Landry, R. L. Ornstein, *J. Phys. Chem. A* **2000**, 104, 7672.
- [25] C.-G. Zhan, D. W. Landry, R. L. Ornstein, *J. Am. Chem. Soc.* **2000**, 122, 2621.
- [26] C.-G. Zhan, D. W. Landry, *J. Phys. Chem. A* **2001**, 105, 1296.
- [27] J. R. Pliego, Jr., J. M. Riveros, *Chem. Phys. Lett.* **2000**, 332, 597.
- [28] J. R. Pliego, Jr., J. M. Riveros, *J. Phys. Chem. A* **2001**, 105, 7241.
- [29] R. H. Nobes, W. J. Bouma, L. Radom, *Chem. Phys. Lett.* **1982**, 89, 497.
- [30] J. A. Pople, M. Head-Gordon, D. J. Fox, K. Raghavachari, L. A. Curtiss, *J. Chem. Phys.* **1989**, 90, 5622.
- [31] L. A. Curtiss, C. Jones, G. W. Trucks, K. Raghavachari, J. A. Pople, *J. Chem. Phys.* **1990**, 93, 2537.
- [32] L. A. Curtiss, K. Raghavachari, G. W. Trucks, J. A. Pople, *J. Chem. Phys.* **1991**, 94, 7221.
- [33] L. A. Curtiss, K. Raghavachari, J. A. Pople, *J. Chem. Phys.* **1993**, 98, 1293.
- [34] J. B. Foresman, T. A. Keith, K. B. Wiberg, J. Snoonian, M. J. Frisch, *J. Phys. Chem.* **1996**, 100, 16098.
- [35] *Gaussian 94*, Revision D.2, M. J. Frisch, G. W. Trucks, H. B. Schlegel, P. M. W. Gill, B. G. Johnson, M. A. Robb, J. R. Cheeseman, T. Keith, G. A. Petersson, J. A. Montgomery, K. Raghavachari, M. A. Al-Laham, V. G. Zakrzewski, J. V. Ortiz, J. B. Foresman, J. Cioslowski, B. B. Stefanov, A. Nanayakkara, M. Challacombe, C. Y. Peng, P. Y. Ayala, W. Chen, M. W. Wong, J. L. Andres, E. S. Replogle, R. Gomperts, R. L. Martin, D. J. Fox, J. S. Binkley, D. J. Defrees, J. Baker, J. P. Stewart, M. Head-Gordon, C. Gonzalez, J. A. Pople, Gaussian, Inc., Pittsburgh PA, **1994**.
- [36] a) J. Tomasi, M. Persico, *Chem. Rev.* **1994**, 94, 2027; b) C. J. Cramer, D. G. Truhlar, *Chem. Rev.* **1999**, 99, 2161. Many other references can also be found in these two reviews.
- [37] P. Claverie, J. P. Daudey, J. Langlet, B. Pullman, D. Piazzola, M. J. Huren, *J. Phys. Chem.* **1978**, 82, 405.
- [38] a) E. S. Marcos, B. Terry, J. L. Rivail, *J. Phys. Chem.* **1985**, 89, 4695; b) E. S. Marcos, R. R. Pappalardo, D. Rinaldi, *J. Phys. Chem.* **1991**, 95, 8928.
- [39] L. C. G. Freitas, R. L. Longo, A. M. Simas, *J. Chem. Soc. Faraday Trans.* **1992**, 88, 189.
- [40] I. Tunon, E. Silla, J. Bertran, *J. Phys. Chem.* **1993**, 97, 5547.
- [41] F. Floris, M. Persico, A. Tani, J. Tomasi, *Chem. Phys.* **1995**, 195, 207.
- [42] A. R. Grimm, G. B. Bacskay, A. D. Haymet, *Mol. Phys.* **1995**, 86, 369.
- [43] I. Tunon, D. Rinaldi, M. F. Ruiz-Lopez, J. L. Rivail, *J. Phys. Chem.* **1995**, 99, 3798.
- [44] a) C. Aleman, S. E. Galembeck, *Chem. Phys.* **1998**, 232, 151; b) C. Aleman, *Chem. Phys. Lett.* **1999**, 302, 461.
- [45] a) I. A. Topol, G. J. Tawa, S. K. Burt, A. A. Rashin, *J. Chem. Phys.* **1999**, 111, 10998; b) P. Bandyopadhyay, M. S. Gordon, *J. Chem. Phys.* **2000**, 113, 1104.
- [46] Experimental values for the enthalpy of formation were taken from NIST Standard Reference Database Number 69—February 2000 Release, to be found under <http://webbook.nist.gov/chemistry/>.
- [47] J. P. Guthrie, *J. Am. Chem. Soc.* **1973**, 95, 6999.
- [48] M. L. Chabiny, S. L. Craig, C. K. Regan, J. I. Brauman, *Science* **1998**, 279, 1882.

Received: October 4, 2001 [F3589]